

coupling method was used to prepare (*S*)-4-phenylmandelic acid from (*S*)-4-bromomandelic acid. The corresponding (*S*)-4-bromomandelic acid was obtained from 4-bromoacetophenone by standard procedures and was resolved with **2**. The substituted phenylethylamines were prepared from the corresponding acetophenones by a standard Leuckardt procedure. A Strecker reaction was used to prepare 4-methylphenylglycine, which was reduced to 4-methylphenylglycinol.

Received: June 5, 2002

Revised: August 15, 2002 [Z19422]

- [1] L. Pasteur, *C. R. Hebd. Seances Acad. Sci.* **1848**, 26, 535.
- [2] a) R. A. Sheldon, *Chirotechnology*, Marcel Dekker, New York, **1993**, chap. 6; b) *Chirality in Industry II* (Eds.: N. A. Collins, G. N. Sheldrake, J. Crosby), Wiley, Chichester, **1997**.
- [3] a) T. Vries, H. Wynberg, E. van Echten, J. Koek, W. ten Hoeve, R. M. Kellogg, Q. B. Broxterman, A. Minnaard, B. Kaptein, S. van der Sluis, L. A. Hulshof, J. Kooistra, *Angew. Chem.* **1998**, 110, 2491; *Angew. Chem. Int. Ed.* **1998**, 37, 2349; b) Eur. Pat. Appl., EP 0,838,448 (to DSM).
- [4] J. Jacques, A. Collet, S. H. Wilen, *Enantiomers, Racemates, and Resolutions*, Wiley, New York, **1981**.
- [5] The cyclic phosphoric acids (P mix) were developed as resolving agents in our lab and have been patented: W. ten Hoeve, H. Wynberg, *J. Org. Chem.* **1985**, 50, 4508; Eur. Pat., 180,276; US Pat., 4,814,477.
- [6] Arthur Conan Doyle, *Silver Blaze*, Strand Magazine, **1892**.
- [7] E. Fogassy, A. Lopata, F. Faigl, F. Darvas, M. Ács, L. Toke, *Tetrahedron Lett.* **1980**, 21, 647.
- [8] Reproducibilities are good; the experimentally determined error limit of the *S* factor is  $\pm 5\%$ .
- [9] Analogous experiments with pure (*S*)-*o*-nitrophenylethylamine (**5**) as the inhibitor led to a *de* value of 51% and an *S* factor of 0.55. With pure (*S*)-*p*-nitrophenylethylamine as the inhibitor the *de* value was 62% and the *S* factor was 0.56. We conclude that use of the more readily available mixture instead of the pure materials is entirely justified and allows direct comparison with the data given in ref. [3].
- [10] In this experiment we used only *o*-nitrophenylethylamine instead of the 1:1 mixture of *o,p* isomers for reasons of simplicity.
- [11] The experimentally determined error limit is  $\pm 0.3^\circ\text{C}$  for this experiment.
- [12] The dissolution temperatures differ somewhat, owing to the high concentrations in this experiment (1.6M); the experimentally determined error limit is  $\pm 0.7^\circ\text{C}$ .
- [13] A manuscript covering the concept of reverse resolutions is in preparation: Dutch Resolution of Alaninol with (*R*)-Mandelic acid by addition of (*S*)- or (*R*)-2-Amino-1-butanol; the Role of Nucleation Inhibition; B. Kaptein, K. L. Pouwer, T. R. Vries, R. F. P. Grimbergen, H. M. J. Grooten, H. L. M. Elsenberg, J. W. Nieuwenhuijzen, R. M. Kellogg, Q. B. Broxterman, *Chem. Eur. J.*, unpublished work.
- [14] a) K. Kinbara, K. Oishi, Y. Harada, K. Saigo, *Tetrahedron* **2000**, 56, 6651; b) K. Kinbara, Y. Harada, K. Saigo, *Tetrahedron: Asymmetry* **1998**, 9, 2219.
- [15] a) L. Addadi, Z. Berkovitch-Yellin, N. Domb, E. Gati, M. Lahav, L. Leiserowitz, *Nature* **1982**, 296, 21; b) Z. Berkovitch-Yellin, L. Addadi, M. Idelson, L. Leiserowitz, M. Lahav, *Nature* **1982**, 296, 27; c) L. Addadi, S. Weinstein, E. Gati, I. Weissbuch, M. Lahav, *J. Am. Chem. Soc.* **1982**, 104, 4610; d) D. Zbaida, M. Lahav, K. Drauz, G. Knaup, M. Kottenhahn, *Tetrahedron* **2000**, 56, 6645.
- [16] K. Sakai, Y. Mackawa, K. Saigo, M. Sukegawa, H. Murakami, H. Nohira, *Bull. Chem. Soc. Jpn.* **1992**, 65, 1747.

## Shape Control of Thermodynamically Stable Cobalt Nanorods through Organometallic Chemistry \*\*

Frédéric Dumestre, Bruno Chaudret,\*

Catherine Amiens, Marie-Claire Fromen, Marie-José Casanove, Philippe Renaud, and Peter Zurcher

The synthesis of nanoparticles is of fundamental importance for the development of novel technologies based on nanomaterials. This is particularly true for magnetic nanomaterials which could be used, amongst other things, for high-density information storage.<sup>[1]</sup> These materials would ideally consist of spatially separated particles in the nanometer range that would function as a single magnetic domain that exhibits ferromagnetic behavior at room temperature, and could be electronically isolated. In addition, the organization of the particles in the solid state or in solution (self-assembly) should be controllable as desired for the intended application.

Several methods are available for the production of magnetic nanomaterials. They can be divided into physical methods, which produce essentially thin layers,<sup>[2,3]</sup> template methods, which involves the growth of nanorods or nanowires by different approaches, frequently electrochemical, within the channels of inorganic or track-etch organic matrixes,<sup>[4]</sup> and chemical methods involving synthesis in a solution of nanoparticles.<sup>[5,6]</sup> The latter may generally allow, after size selection, the formation of self-assembled superlattices. Sun and Murray<sup>[5]</sup> have, for example, recently reported a high-temperature preparation of 9 nm cobalt nanoparticles displaying a long-range self-organization. This method has been extended to the synthesis of Fe/Pt particles to increase the magnetic anisotropy of the materials, with the goal of producing high-density memories.<sup>[7]</sup> Self-organized cobalt nanoparticles have also been reported by the group of Pileni by reverse micelle synthesis.<sup>[8]</sup>

In all cases, as a result of their small dimension, the particles are superparamagnetic at room temperature and thus not usable for many applications, such as magnetic recording. One way to increase the magnetic anisotropy of the particles is to modify their shape. This problem has been addressed by Alivisatos who initially demonstrated the importance of reaction conditions, in particular the concentration of the

[\*] Dr. B. Chaudret, F. Dumestre, Dr. C. Amiens  
Laboratoire de Chimie de Coordination du CNRS  
205, route de Narbonne, 31077 Toulouse Cédex 04 (France).  
Fax: (+33) 5-61-55-30-03  
E-mail: chaudret@lcc-toulouse.fr

F. Dumestre, Dr. P. Renaud  
Digital DNA Labs, Semiconductor Products Sector, Motorola  
le Mirail B.P. 1029, 31023 Toulouse Cédex (France)  
M.-C. Fromen, Dr. M.-J. Casanove  
CEMES-CNRS  
29 Rue Marvig, BP 4347, F 31055 Toulouse, France.

Dr. P. Zurcher  
Digital DNA Labs, Semiconductor Products Sector, Motorola  
2100 E. Elliot Road, Tempe, AZ-85824 (USA)

[\*\*] The authors thank CNRS and MOTOROLA S.P.S. for support, M. Vincent Collière, Lucien Datas, and TEMSCAN service (Université Paul Sabatier Toulouse) for transmission electron microscopy.

precursors and the ratio of surfactants, for preparing CdSe nanocrystals of various shapes including nanorods.<sup>[9]</sup> The same methodology was employed for synthesizing cobalt nanorods, which were found to be thermodynamically unstable and to rearrange into spherical particles.<sup>[10]</sup> This result contrasts with a recent report by Hyeon and co-workers, who show that spherical iron nanoparticles may be used at 320 °C as initiators for the growth of nanorods.<sup>[11]</sup> However, no systematic study on the influence of ligand-type on the particle aspect ratio, and hence on the magnetic properties of prepared metal nanoparticles, has been reported so far.

In our group we have previously described the synthesis of magnetic nanoparticles using olefinic complexes as precursors.<sup>[12,13]</sup> These compounds rapidly decompose to give alkane by-products which do not interact with the surface of the particles under the reaction conditions. This methodology allows the synthesis of magnetic nanoparticles that display the same magnetic moment as particles of similar size in the gas phase.<sup>[14]</sup> The absence of oxidation and of strongly coordinating ligands at the surface of the particles may also favor size and shape changes in solution, as recently demonstrated for ruthenium,<sup>[15]</sup> and therefore an easier control of these parameters by the surrounding medium. In separate studies, we have emphasized the role of amines for the formation of nanorods or nanowires.<sup>[16]</sup> This technique has been used to produce nickel nanorods, the surface magnetism of which is not altered by the presence of amine ligands.<sup>[17]</sup>

In this paper we describe the synthesis and magnetic properties of novel cobalt nanoparticles. We demonstrate that by varying the synthesis parameters it is possible to selectively prepare spherical nanoparticles of uniform size, nanorods, the aspect ratio of which is controlled by the alkyl chain-length of the ligand, or even very long nanowires. Finally, we report the magnetic properties of these nanoparticle materials.

The decomposition reactions of  $[\text{Co}(\eta^3\text{-C}_8\text{H}_{13})(\eta^4\text{-C}_8\text{H}_{12})]^{[18]}$  were carried out in anisole under a pressure of 3 bar  $\text{H}_2$  (initial pressure at room temperature in the reactor) in the presence of ligands. The use of a single ligand such as hexadecylamine (1:1 Co/amine molar ratio) leads to small, agglomerated nanoparticles at room temperature. Similarly, the use of oleylamine ( $\text{CH}_3(\text{CH}_2)_7\text{CH}=\text{CH}(\text{CH}_2)_8\text{NH}_2$ ) at 150 °C produces particles that display a large size distribution, whereas monodisperse particles with a mean size of 5 nm are obtained when using oleic acid under the same conditions (sample 1). These particles self-organize on a microscopy grid into 2D and 3D crystalline arrays. When both oleic acid and oleylamine are used as ligands (1 equivalent each, 150 °C, and 3 bar  $\text{H}_2$ , standard conditions), the synthesis initially produces nanoparticles with mean dimensions of approximately 3 nm, as shown by

transmission electron microscopy (TEM, sample 2; Figure 1 A), which are the only species present after reacting for 3 h. However, after 48 h, regular nanorods of approximately  $9 \times 40$  nm are the unique species in solution (sample 3; Figure 1 B). To determine the importance of dihydrogen, two parallel reactions were carried out. In both cases the precursor was decomposed under standard conditions. After 3 h the reactors were evacuated, and the first reactor was pressurized again to 3 bar with  $\text{H}_2$  whereas the second reactor was placed under argon. After 48 h nanorods were found in the first reactor and 4 nm nanoparticles in the second. The nature of the precursor complex is also important since, under standard conditions, the use of  $[\text{Co}_2(\text{CO})_8]$  in place of  $[\text{Co}(\eta^3\text{-C}_8\text{H}_{13})(\eta^4\text{-C}_8\text{H}_{12})]$  leads to polydisperse particles with a mean size of approximately 10 nm. The role of the ligands, with particular respect to the concentration of oleic acid and the nature of the amine, was then examined in order to understand the formation of the particles. If the oleic acid concentration was decreased (0.3 equivalents, with respect to Co), particles of regular size (approximately 3 nm) were formed, whereas if the concentration was doubled (2 equivalents), very long (micron range) nanowires of 4 nm diameter were produced (sample 4; Figure 1 C). Replacing oleylamine by octyl-, dodecyl-, hexadecyl-, and octadecylamine causes a dramatic change in the dimensions of the nanorods that are produced (Figure 2). The use of octadecylamine yields nanorods of comparable size, but with greater regularity, to those obtained with oleylamine ( $47 \times 6$  nm, Figure 2 C); hexadecylamine produces longer and thinner rods ( $120 \times 5.5$  nm, Figure 2 E) whereas octylamine yields smaller and wider ones ( $17 \times 10$  nm, Figure 2 F). Therefore, particles displaying aspect ratios between 1.7 and 22 can be controlled solely by the number of carbon atoms in the alkyl chain of the amine, whereas a very large aspect ratio may be obtained for the nanowires prepared in the presence of excess oleic acid. The variation of the length and diameter of the produced nanorods is summarized in Figure 2 A, 2 B.

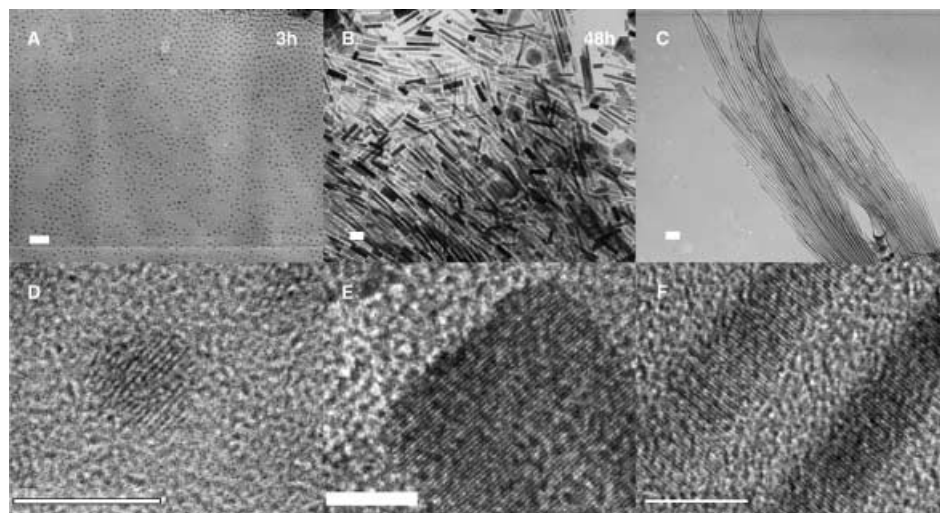


Figure 1. Variation of size and shape with reaction time and the ratio of stabilizing agents. A, B) TEM micrographs of nanoparticles and nanorods obtained with 1 mmol of oleylamine and 1 mmol of oleic acid after 3 h and 48 h, respectively; Bar = 30 nm; C) TEM micrograph of nanowires obtained with 1 mmol of oleylamine and 1 mmol of oleic acid after 48 h; Bar = 30 nm; D, E, F) High resolution (HR)TEM images of the nanoparticles, nanorods, and nanowires presented in A, B, and C, respectively; Bar = 5 nm.

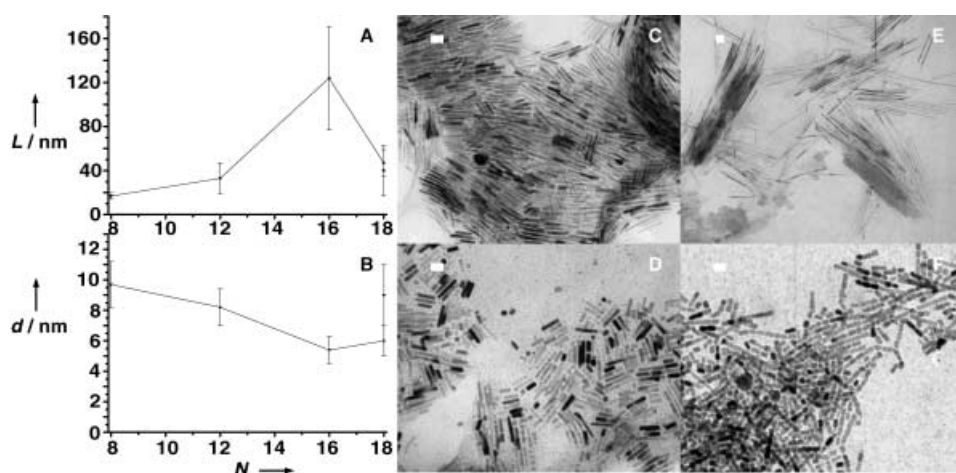


Figure 2. Variation of the aspect ratio of nanorods with respect to the change in the alkyl chain length of the amine. A) Evolution of nanorod length; B) Evolution of nanorod diameter; C–F) TEM micrographs of hcp cobalt nanorods obtained with oleic acid and octadecylamine, dodecylamine, hexadecylamine, and octylamine, respectively: Bar = 30 nm.

These results demonstrate the possibility to selectively synthesize nanorods, but raise questions concerning the exact growth mechanism and, in particular, the exact role of the ligands. It has been previously proposed that the growth mechanism of nanorods could be related to the preferred coordination of the ligand along a face of a growing crystal.<sup>[6,10,19]</sup> In the present case, the employed amine ligands display similar chemical properties, in terms of basicity and affinity for the metal, but form very different nanoobjects. This suggests that, in the present case, the nanorod synthesis is controlled by supramolecular organization and/or the dynamics of the ligands in solution; it is conceivable that longer alkyl chains could organize across longer distances. Oleylamine displays a “cis” configuration, which leads to an apparent rod length comparable to that of octylamine, with less opportunity for long-range organization; this could be a reason for the relatively low regularity of the rods obtained in this case. Oleic acid can also play an important role in this organization since its concentration relative to the amine has a strong influence on the aspect ratio of the nanoobjects produced. In addition, it presumably transforms rapidly in the medium into the oleate anion by deprotonation in the presence of amines, which may lead to a strongly associated medium and/or coordination to cobalt. The necessity of dihydrogen for the synthesis of rods from nanospheres probably arises from the necessity to remove the carboxylate groups from the surface to allow coalescence and growth to occur. This, therefore, suggests a strong coordination of oleate anions to the nanoparticles formed at the early stage of the reaction.<sup>[20]</sup>

All of the particles, rods, and wires described above consist of a pure hexagonal close-packed (hcp) cobalt structure, which displays no sign of oxidation as evidenced by wide-angle X-ray scattering (WAXS) and high-resolution electron microscopy (HREM) studies. The rods and wires are monocrystalline and adopt the  $c$  axis of the hcp structure as the growth axis. Magnetic measurements were carried out on all samples, in particular the 3 nm nanoparticles obtained after 3 h under standard conditions (sample 2) and nanorods produced after 48 h under the same conditions (sample 3).

The former are superparamagnetic at room temperature with a blocking temperature of 20 K, whereas the latter are ferromagnetic at room temperature. Hysteresis loop measurements at 2 K record, for both samples, a saturation magnetization ( $M_s$ ) of  $160 \text{ A m}^2 \text{ kg}_{\text{Co}}^{-1}$ , which corresponds to a magnetic moment per atom of  $\mu = 1.71 \mu_B$ , identical to that found in bulk cobalt. In addition, a coercive field ( $H_c$ ) of respectively 1100 and 8900 Oe is found for samples 2 and 3, hence demonstrating the importance of the shape anisotropy in such systems (see Figure 3).

This work emphasizes the role of the organometallic precursor in the synthesis of the nanomaterial. The high decomposition rate of the precursor and, more importantly, the absence of by-products that could potentially interact with the surface allows the particles to grow without losing their intrinsic magnetic properties.

These objects display a saturation magnetization per cobalt atom that is identical or very close to that of bulk cobalt, which is consistent with the pure  $\sigma$ -donor behavior of both the amine and the acid ligands.<sup>[14,17]</sup> Furthermore, their magnetic

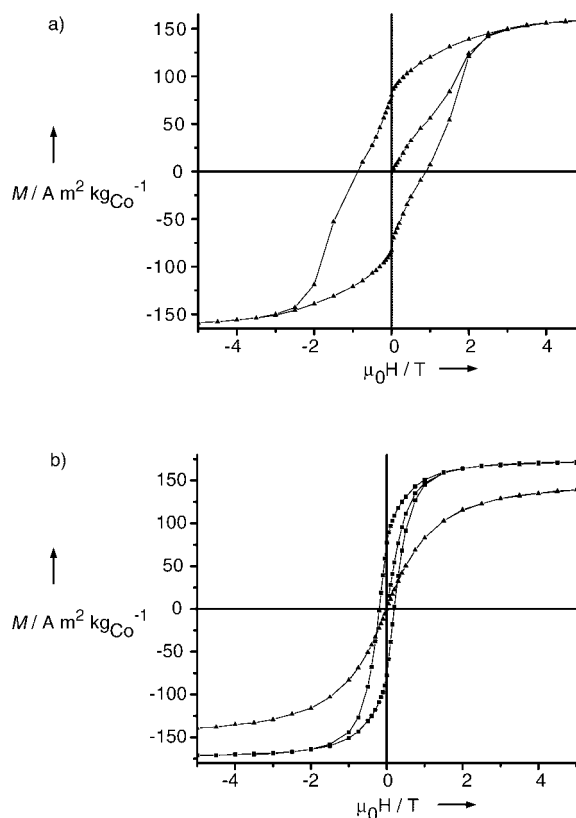


Figure 3. Plots of magnetization against applied magnetic field. a) Hysteresis loop of cobalt nanorods obtained with 1 mmol of oleylamine and 1 mmol of oleic acid: (▲) measured at 300 K. b) Hysteresis loops of cobalt nanoparticles obtained with 1 mmol of oleylamine and 1 mmol of oleic acid: (■) measured at 2 K, (▲) measured at 300 K.

anisotropy may be controlled by their aspect ratio, which gives rise to ferromagnetic nanomaterials at room temperature. The rods grow after the initial formation of spherical nanoparticles; the exact mechanism of this process is not known but we note that the initial formation of nanoparticles, followed by formation of nanorods or nanowires either through coalescence of the initial particles<sup>[21]</sup> or upon using the particles as nuclei for an anisotropic growth process, have been very recently reported.<sup>[22]</sup> Further work will be necessary to determine the exact mechanism that operates in our case.

In conclusion, we describe in this report a new and simple method for the preparation of cobalt nanoparticles, nanorods, and nanowires of uniform diameter that does not require a special procedure or size selection. The magnetic nanowires have no equivalent, whereas the rods differ from those previously described by their uniformity of diameter, their thermodynamic stability, and the possibility of fine tuning of their aspect ratio. We further demonstrate that, under these conditions, the nanomaterials maintain a magnetization at saturation similar to bulk cobalt. This results from the choice of ligands that do not display  $\pi$ -accepting behavior, which is in agreement with previous research work from our group. All of these aspects emphasize the role of an organometallic approach in the design of precursors and ligands. Finally, these objects may find use in many practical applications such as, for example, in data storage.

Received: July 10, 2002

Revised: September 3, 2002 [Z19713]

- [1] D. Weller, A. Moser, *IEEE Trans. Magn.* **1999**, 35, 4423.
- [2] Y. M. Kim, D. Choi, K. H. Kim, S. H. Han, H. J. Kim, *IEEE Trans. Magn.* **2001**, 37, 2288.
- [3] M. Dumm, M. Zölfl, R. Moosbühler, M. Brockmann, T. Schmidt, G. Bayreuther, *J. Appl. Phys.* **2000**, 87, 5457.
- [4] H. Cao, Z. Xu, H. Sang, D. Sheng, C. Tie, *Adv. Mater.* **2001**, 13, 121.
- [5] S. Sun, C. B. Murray, *J. Appl. Phys.* **1999**, 85, 4325.
- [6] V. F. Puentes, K. M. Krishnan, A. P. Alivisatos, *Appl. Phys. Lett.* **2001**, 78, 2187.
- [7] S. Sun, C. B. Murray, D. Weller, L. Folks, A. Moser, *Science* **2000**, 287, 1989.
- [8] J. Legrand, A. T. Ngo, C. Petit, M. P. Pileni, *Adv. Mater.* **2001**, 13, 58.
- [9] L. S. Li, J. Hu, W. Yang, A. P. Alivisatos, *Nano Lett.* **2001**, 1, 349.
- [10] V. F. Puentes, K. M. Krishnan, A. P. Alivisatos, *Science* **2001**, 291, 2115.
- [11] J. Park-Sang, K. Seungsoo, S. Lee, Z. G. Khim, K. Char, T. Hyeon, *J. Am. Chem. Soc.* **2000**, 122, 8581.
- [12] T. Ould Ely, C. Amiens, B. Chaudret, E. Snoeck, M. Verelst, M. Respaud, J. M. Broto, *Chem. Mater.* **1999**, 11, 526.
- [13] M. Verelst, T. Ould Ely, C. Amiens, E. Snoeck, P. Lecante, A. Mosset, M. Respaud, J. M. Broto, B. Chaudret, *Chem. Mater.* **1999**, 11, 2702.
- [14] M. Respaud, J. M. Broto, H. Rakoto, A. R. Fert, L. Thomas, B. Barbara, M. Verelst, E. Snoeck, P. Lecante, A. Mosset, J. Osuna, T. Ould Ely, C. Amiens, B. Chaudret, *Phys. Rev. B* **1998**, 57, 2925.
- [15] C. Pan, K. Pelzer, K. Philippot, B. Chaudret, F. Dassenoy, P. Lecante, M. J. Casanove, *J. Am. Chem. Soc.* **2001**, 123, 7584.
- [16] K. Soulantica, A. Maisonnat, F. Senocq, M. C. Fromen, M. J. Casanove, B. Chaudret, *Angew. Chem.* **2001**, 113, 3071; *Angew. Chem. Int. Ed.* **2001**, 40, 2983.
- [17] N. Cordente, M. Respaud, F. Senocq, M. J. Casanove, C. Amiens, B. Chaudret, *Nano Lett.* **2001**, 1, 565.
- [18] S. Otsuka, M. Rossi, *J. Chem. Soc. A* **1968**, 2630.
- [19] Z. A. Peng, X. Peng, *J. Am. Chem. Soc.* **2001**, 123, 1389.
- [20] J. S. Bradley, B. Tesche, W. Busser, M. Maase, M. Reetz, *J. Am. Chem. Soc.* **2000**, 122, 4631.
- [21] Z. Tang, N. A. Kotov, M. Giersig, *Science* **2002**, 297, 237.
- [22] Z. A. Peng, X. Peng, *J. Am. Chem. Soc.* **2002**, 124, 3343.

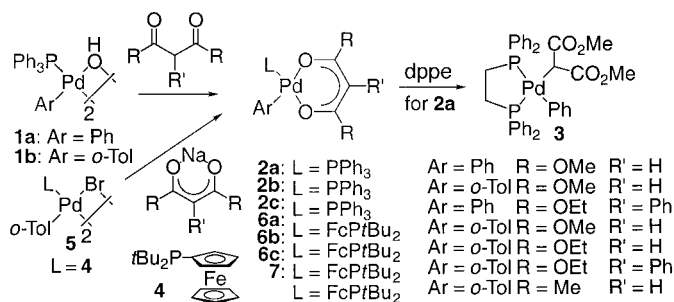
## Generation of Reactivity from Typically Stable Ligands: C–C Bond-Forming Reductive Elimination from Aryl Palladium(II) Complexes of Malonate Anions\*\*

Joanna P. Wolkowski and John F. Hartwig\*

Anions of 1,3-dicarbonyl compounds are some of the most common ligands in transition-metal chemistry.<sup>[1,2]</sup> They typically bind in an  $\eta^2$ -O,O fashion,<sup>[3]</sup> have delocalized charge, and donate electron density more weakly to a metal center than alkyls or alkoxides. They are usually supporting ligands that are ancillary to the site of reaction. Anions of 1,3-dicarbonyl compounds are also common nucleophiles in metal-catalyzed allylic substitution,<sup>[4–6]</sup> but the facility of this chemistry relies on external attack of the anion without coordination to the metal center. If metal fragments could induce reactivity from coordinated versions of these anions, then complexes of these common ligands could serve as intermediates in catalytic processes.

Complexes of malonate anions are likely intermediates in recently developed palladium-catalyzed arylations of malonates.<sup>[7–11]</sup> Although palladium complexes of malonate anions have been isolated previously,<sup>[12–16]</sup> their reactivity has been limited.<sup>[17–20]</sup> We report here reductive elimination of arylmalonate and acetylarylaceton from isolated aryl palladium complexes of malonate and acetylaceton anions, respectively. Our results suggest that the propensity of these complexes to undergo reductive elimination depends critically on the steric properties of the ancillary phosphane ligand.

Our synthesis of aryl palladium malonates is summarized in Scheme 1. Addition of dimethyl malonate or diethyl phenylmalonate to the basic  $\text{PPh}_3$ -ligated palladium hydroxide dimers **1a**<sup>[21,22]</sup> and **1b** generated the O,O'-bound palladium dimethyl malonate complexes **2a–c**. Complexes **2a** and **2c** were characterized by X-ray diffraction (Figure 1). No unusual angles at the palladium center were found in **2a** or



Scheme 1. Synthesis of aryl palladium malonates.

[\*] Prof. J. F. Hartwig, J. P. Wolkowski  
Department of Chemistry  
Yale University  
P.O. Box 208107, New Haven, CT 06520-8107 (USA)  
Fax: (+1) 203-432-3917  
E-mail: john.hartwig@yale.edu

[\*\*] We thank the National Institutes of Health for support of this work (GM-58108) and Johnson-Matthey for a gift of palladium salts.

Supporting information for this article is available on the WWW under <http://www.angewandte.org> or from the author.